Linearity by Synthesis: An Intrinsically Linear AlGaN/GaN-on-Si Transistor with OIP3/(F-1)P_{DC} of 10.1 at 30 GHz

Woojin Choi[1], Venkatesh Balasubramanian[2], Peter M. Asbeck[1], and Shadi A. Dayeh[1*]
[1]Department of Electrical and Computer Engineering, University of California San Diego, CA, 92093, USA.
[2]Maury Microwave Corporation, Ontario, California 91764, USA
*Email: sdayeh@eng.ucsd.edu

Introduction In today's radio-frequency (RF) systems, linearity of amplifiers is a key concern due to presence of significant numbers of in-band interferers in the crowded spectrum. GaN high electron mobility transistors (HEMTs) can provide low noise front-end amplifiers, but state-of-the-art GaN HEMTs still possess non-linearity exhibited by a transconductance, g_m, roll-off from its peak due to the dynamic source access resistance and other factors [1]. The dynamic range figure-of-merit (DRFOM) for low noise amplifiers (LNAs) [2], OIP3/(F-1)P_{DC}, where OIP3 is the output 3rd-order intercept point (OIP3), P_{DC} is the DC power, and F is the noise factor, is still limited to ~1.7 in mm-wave GaN transistors [3]. Joglekar et al. attempted to increase linearity by using different Fin widths resulted in flat g_m of ~2 V [1]; linearity figures of merit were not properly assessed. Here, we demonstrate a novel method to synthesize g_m plateau over a 6 V gate overdrive and a record DRFOM of 10.1 in GaN HEMTs at 30 GHz.

Experiment and Device Design The metal-insulator-semiconductor (MIS) structure incorporates a planar FET in parallel with a set of fin FETs. A commercial $Al_{0.23}Ga_{0.77}N$/GaN-on-Si wafer was used without additional epitaxial layer growth. An alloyed Ti/Al-based Ohmic contact was used and Fin structures were formed by e-beam lithography and dry etching. Fin widths (W_{Fin}) were varied from 50 nm to 200 nm, and fin length (L_{Fin}), gap between Fins (W_{gap}), and mesa width (W_M) were fixed at 150 nm, 200 nm, and 20 µm, respectively. A 6 nm-thick Al_2O_3 was deposited by atomic layer deposition (ALD), and a Ti/Au gate metal was evaporated. After opening ohmic windows, Ti/Au pads and Si_3N_4 passivation layers were deposited. The gate-to-source (L_{GS}), gate-to-drain distances (L_{GD}), and a gate length (L_G) were 0.5 µm, 1.35 µm, and 90 nm, respectively. Figure 1 shows the cross-sectional transmission electron microscopy (TEM) image of the fabricated Fin metal-insulator-semiconductor (MIS) structure.

In Fin MIS-HEMTs, as shown in Figure 2, threshold voltages (V_T) shift in positive direction with decreasing W_{Fin}, because of the tri-gate structure [4]. For a device composed of a planar and several Fin channels, termed a synthesized device, I_D can be expressed as: $I_{D,total}(V_{GS}) = \alpha_0 I_{D,0}(V_{GS} - V_{T,0}) + \alpha_1 I_{D,1}(V_{GS} - V_{T,1}) + \cdots + \alpha_k I_{D,k}(V_{GS} - V_{T,k})$, where α_k is the weight of k^{th} channels for a family of Fins with a width, $W_{Fin,k}$, and a threshold voltage, $V_{T,k}$. k=0 represents the planar device characteristics. We chose 4 different W_{Fin} of 160, 100, 80, and 50 nm to linearize the transfer characteristic of the planar device. As shown in Figure 3, we exploited g_m' for the selected W_{Fin} and computed α_k to obtain a wide zero g_m' window for V_{GS} from -4 V to 2 V. Figure 4 shows a scanning electron microscopy (SEM) image of the fabricated synthesized device. Figure 5(a) and (b) are the linearized transfer characteristic showing a g_m plateau of ~6 V and the output characteristics, respectively. Figure 6 shows measured g_m and its derivatives with multiple g_m'' sweet spots.

LNA Performance at 30 GHz The planar-Fin synthesis design was adapted to another device with 8-fingers, 90 nm T-gates, a shorter L_{GS} of 250 nm, and L_{GD} of 350 nm on the same die for mm-wave LNAs. The device was biased at V_{DS}=3 V and I_D=63 mA in the following single-tone continuous wave (CW) power sweep and two-tone linearity measurements at 30 GHz at Maury Microwave with the source and load impedances matched to Γ_{in}^* and $0.17\angle 140°$, respectively. As can be seen in Figure 7(a), the single-tone CW power sweep measurement shows maximum output power (P_{out}), linear gain, and peak power added efficiency (PAE) of 19.6 dBm, 7.52 dB, and 32.3 %, respectively. Figure 7(b) shows the measured distortions to amplitude (AM-AM ($|S_{21}|$)), and to phase (AM-PM ($\measuredangle S_{21}$)). The output 1-dB gain compression point (P_{1dB}) was as high as 17.8 dBm. The AM-PM distortion was only 0.3 degree at P_{1dB}. As shown in Figure 8(a), the input 3rd-order intercept point (IIP3) of 23.5 dBm and OIP3 of 31 dBm were extrapolated at a P_{DC} of 189 mW. The ratio of carrier-to-IM3 (C/IM3) was above 45 dBc at P_{in} per tone of 0 dBm. On-wafer noise measurement was also carried out with frequencies from 8 to 50 GHz. The minimum noise figure (NF_{min}) and the associated gain (G_a) are shown in Figure 8(b), and the NF_{min} was 2.2 dB at 30 GHz, resulting in the LNA FOM of 10.1. To the best of our knowledge, this value is the record in GaN-based devices.

Conclusion The concept of an intrinsically synthesizable linear device is demonstrated. It was implemented by changing only the device layout; additional performance gains can be attained by further materials engineering.

Acknowledgement The authors acknowledge the support of Renjie Chen for TEM, nano3 and Center for Integrated Nanotechnologies (CINT). This work was supported in part by an NSF-ECCS award #1711030.

References

[1] S. Joglekar *et al.*, *IEDM Tech. Dig.*, p. 613, (2017).
[2] V. Aparin *et al.*, *IEEE TMTT*, p. 571, (2005).
[3] M. Micovic *et al.*, *CSICS Tech. Dig.*, p.1, (2016).
[4] J. Ma *et al.*, *IEEE TED*, vol. 66, p. 4068, (2019).

978-1-7281-7047-3/20/$31.00 ©2020 IEEE

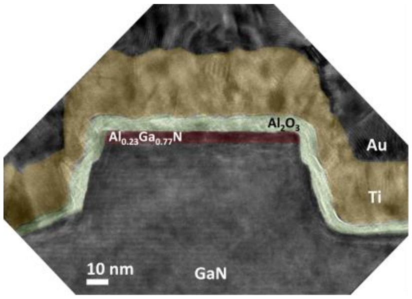

Fig. 1 A cross-sectional TEM image of the fabricated Fin MIS-HEMTs.

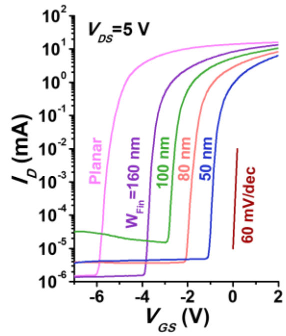

Fig. 2 Transfer characteristics in log-scale with varying Fin widths.

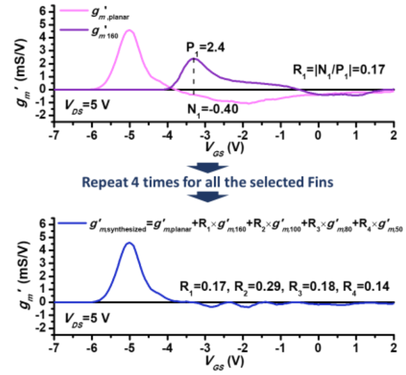

Fig. 3 Linearization of transfer characteristics by using g_m'-V_{GS}.

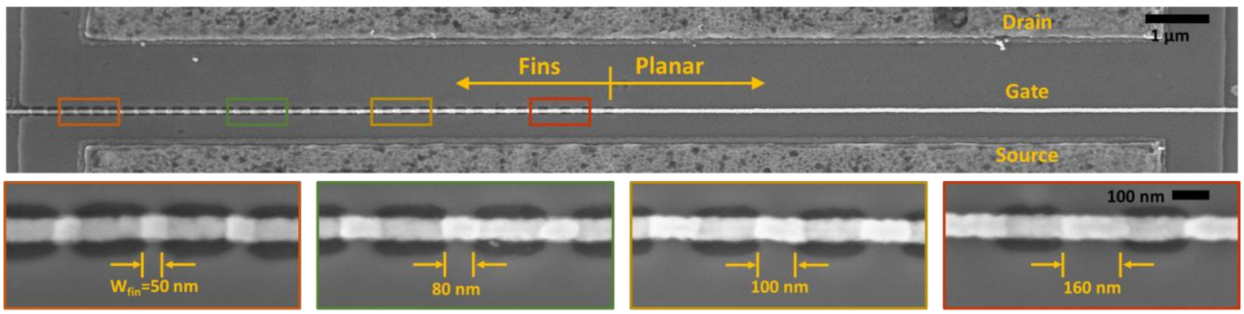

Fig. 4 A SEM image of the synthesized device consisting of planar and multi-Fin regions.

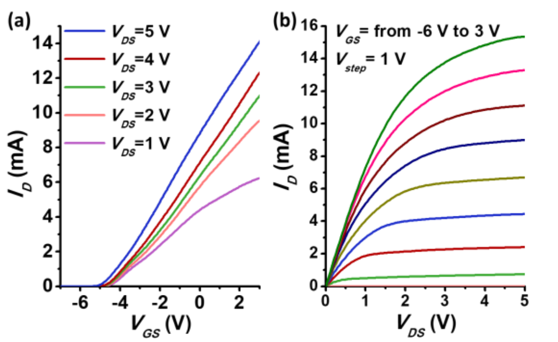

Fig. 5 Measured transfer characteristics of the fabricated synthesized device.

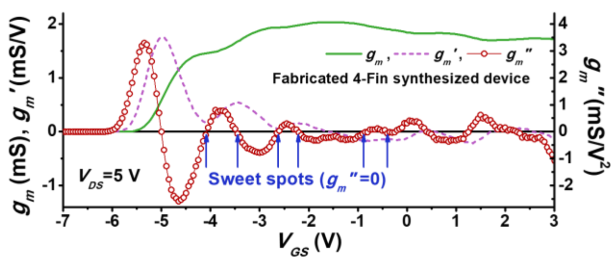

Fig. 6 g_m, g_m', and g_m'' characteristics with respect to V_{GS}. Multiple 'sweet spots' were observed.

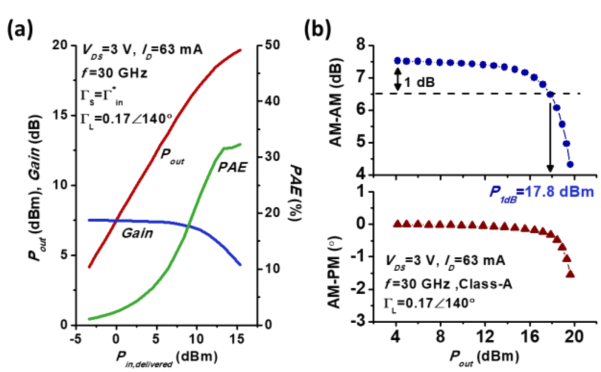

Fig. 7 The single-tone CW power sweep and distortions to amplitude (AM-AM) and phase (AM-PM) results.

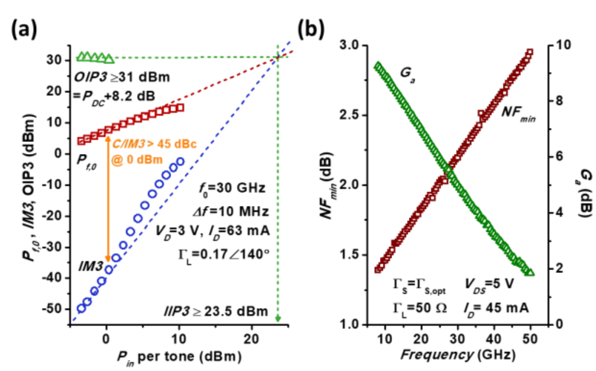

Fig. 8 The two-tone linearity and noise measurements characteristics for the synthesized device.

978-1-7281-7047-3/20/$31.00 ©2020 IEEE